Unveil the transcriptome alteration of POMC neuron in diet-induced obesity

Peng Lyu
Fuzhou University College of Biological Science and Engineering
Zhishun Huang
Fuzhou University College of Biological Science and Engineering
Qingjun Feng
Fuzhou University College of Biological Science and Engineering
Yongfu Su
Fuzhou University College of Biological Science and Engineering
Mengying Zheng
Fuzhou University College of Biological Science and Engineering
Yannv Hong
Fuzhou University College of Biological Science and Engineering
Xiang Cai
Fuzhou University College of Biological Science and Engineering
Zhonglei LU (zhonglei.lu@fzu.edu.cn)
Fuzhou University College of Biological Science and Engineering https://orcid.org/0000-0002-8915-4828

Research article

Keywords: High-Fat-Diet (HFD), Diet-Induced Obesity (DIO), POMC neuron, Neuron homeostasis, pRb phosphorylation

Posted Date: December 19th, 2019

DOI: https://doi.org/10.21203/rs.2.19329/v1

The ARRIVE Guidelines Checklist

Animal Research: Reporting In Vivo Experiments

Carol Kilkenny[1], William J Browne[2], Innes C Cuthill[3], Michael Emerson[4] and Douglas G Altman[5]

[1]The National Centre for the Replacement, Refinement and Reduction of Animals in Research, London, UK, [2]School of Veterinary Science, University of Bristol, Bristol, UK, [3]School of Biological Sciences, University of Bristol, Bristol, UK, [4]National Heart and Lung Institute, Imperial College London, UK, [5]Centre for Statistics in Medicine, University of Oxford, Oxford, UK.

	ITEM	RECOMMENDATION	Section/ Paragraph
Title	1	Provide as accurate and concise a description of the content of the article as possible.	Title/ Page 1
Abstract	2	Provide an accurate summary of the background, research objectives, including details of the species or strain of animal used, key methods, principal findings and conclusions of the study.	Abstract/ Page 1-2
INTRODUCTION			
Background	3	a. Include sufficient scientific background (including relevant references to previous work) to understand the motivation and context for the study, and explain the experimental approach and rationale. b. Explain how and why the animal species and model being used can address the scientific objectives and, where appropriate, the study's relevance to human biology.	Background / Paragragh 3
Objectives	4	Clearly describe the primary and any secondary objectives of the study, or specific hypotheses being tested.	Background/ Paragragh 4
METHODS			
Ethical statement	5	Indicate the nature of the ethical review permissions, relevant licences (e.g. Animal [Scientific Procedures] Act 1986), and national or institutional guidelines for the care and use of animals, that cover the research.	Method/ Paragragh 1
Study design	6	For each experiment, give brief details of the study design including: a. The number of experimental and control groups. b. Any steps taken to minimise the effects of subjective bias when allocating animals to treatment (e.g. randomisation procedure) and when assessing results (e.g. if done, describe who was blinded and when). c. The experimental unit (e.g. a single animal, group or cage of animals). A time-line diagram or flow chart can be useful to illustrate how complex study designs were carried out.	a. Method/ Paragragh 2 b. Method/ Paragragh 2 c. Method/ Paragragh 2
Experimental procedures	7	For each experiment and each experimental group, including controls, provide precise details of all procedures carried out. For example: a. How (e.g. drug formulation and dose, site and route of administration, anaesthesia and analgesia used [including monitoring], surgical procedure, method of euthanasia). Provide details of any specialist equipment used, including supplier(s). b. When (e.g. time of day). c. Where (e.g. home cage, laboratory, water maze). d. Why (e.g. rationale for choice of specific anaesthetic, route of administration, drug dose used).	a. Method/ Paragragh 2 b. Method/ Paragragh 2 c. Method/ Paragragh 2
Experimental animals	8	a. Provide details of the animals used, including species, strain, sex, developmental stage (e.g. mean or median age plus age range) and weight (e.g. mean or median weight plus weight range). b. Provide further relevant information such as the source of animals, international strain nomenclature, genetic modification status (e.g. knock-out or transgenic), genotype, health/immune status, drug or test naïve, previous procedures, etc.	a. Method/ Paragragh 2 b. Method/ Paragragh 2 c. Method/ Paragragh 2

The ARRIVE guidelines. Originally published in *PLoS Biology*, June 2010[1]

Housing and husbandry	9	Provide details of: a. Housing (type of facility e.g. specific pathogen free [SPF]; type of cage or housing; bedding material; number of cage companions; tank shape and material etc. for fish). b. Husbandry conditions (e.g. breeding programme, light/dark cycle, temperature, quality of water etc for fish, type of food, access to food and water, environmental enrichment). c. Welfare-related assessments and interventions that were carried out prior to, during, or after the experiment.	a. Method/ Paragragh 2 b. Method/ Paragragh 2 c. Method/ Paragragh 2
Sample size	10	a. Specify the total number of animals used in each experiment, and the number of animals in each experimental group. b. Explain how the number of animals was arrived at. Provide details of any sample size calculation used. c. Indicate the number of independent replications of each experiment, if relevant.	Method/ Paragraph 2-3
Allocating animals to experimental groups	11	a. Give full details of how animals were allocated to experimental groups, including randomisation or matching if done. b. Describe the order in which the animals in the different experimental groups were treated and assessed.	Method/ Paragraph 2
Experimental outcomes	12	Clearly define the primary and secondary experimental outcomes assessed (e.g. cell death, molecular markers, behavioural changes).	Method/ Paragragh 3
Statistical methods	13	a. Provide details of the statistical methods used for each analysis. b. Specify the unit of analysis for each dataset (e.g. single animal, group of animals, single neuron). c. Describe any methods used to assess whether the data met the assumptions of the statistical approach.	Method/ Statistic analysis Page 15
RESULTS			
Baseline data	14	For each experimental group, report relevant characteristics and health status of animals (e.g. weight, microbiological status, and drug or test naïve) prior to treatment or testing. (This information can often be tabulated).	Results/ Paraprагh 1
Numbers analysed	15	a. Report the number of animals in each group included in each analysis. Report absolute numbers (e.g. 10/20, not 50%[2]). b. If any animals or data were not included in the analysis, explain why.	Results/ Paraprагh 1
Outcomes and estimation	16	Report the results for each analysis carried out, with a measure of precision (e.g. standard error or confidence interval).	Results/ Paraprагh 1
Adverse events	17	a. Give details of all important adverse events in each experimental group. b. Describe any modifications to the experimental protocols made to reduce adverse events.	N/A
DISCUSSION			
Interpretation/ scientific implications	18	a. Interpret the results, taking into account the study objectives and hypotheses, current theory and other relevant studies in the literature. b. Comment on the study limitations including any potential sources of bias, any limitations of the animal model, and the imprecision associated with the results[2]. c. Describe any implications of your experimental methods or findings for the replacement, refinement or reduction (the 3Rs) of the use of animals in research.	Disccusion/ Paragraph 1-3
Generalisability/ translation	19	Comment on whether, and how, the findings of this study are likely to translate to other species or systems, including any relevance to human biology.	Disccusion/ Conclusion Page 12
Funding	20	List all funding sources (including grant number) and the role of the funder(s) in the study.	Declarations /Funding

References:
1. Kilkenny C, Browne WJ, Cuthill IC, Emerson M, Altman DG (2010) Improving Bioscience Research Reporting: The ARRIVE Guidelines for Reporting Animal Research. *PLoS Biol* 8(6): e1000412. doi:10.1371/journal.pbio.1000412
2. Schulz KF, Altman DG, Moher D, the CONSORT Group (2010) CONSORT 2010 Statement: updated guidelines for reporting parallel group randomised trials. *BMJ* 340:c332.

Unveil the transcriptome alteration of POMC neuron in diet-induced obesity

Peng Lyu*, Zhishun Huang*, Qingjun Feng, Yongfu Su, Mengying Zheng, Yannv Hong, Xiang Cai Zhonglei Lu#

1. College of Biological Science and Technology, Fuzhou University, Fuzhou, China, 350108

* These authors contributed equally to this work.

Authors to whom correspondence: Prof. Zhonglei Lu; College of Biological Science and Technology, Fuzhou University, Fuzhou, China, 350108; Phone: 13205021363; Email: zhonglei.lu@fzu.edu.cn

Abstract

Background: Loss of neuron homeostasis in the Arcuate nucleus (ARC) is suggested to be responsible for the development diet-induced-obesity (DIO). We previously reported that loss of *Rb1* gene compromised the homeostasis of anorexigenic POMC neurons in ARC and induced obesity in mice. Method: To shed light on how DIO develops, we propose to analyze the transcriptomic alteration of POMC neurons in mice following high fat die (HFD) feeding. We isolated the POMC neurons from established DIO mice and performed transcriptomic profiling on them by RNA-seq.

Results: A total of 1,066 genes (628 up-regulated and 438 down-regulated) were identified as differentially expressed genes (DEGs). Pathway enrichment analysis with these DEGs further revealed that 'cell cycle', 'apoptosis', 'chemokine signalling' and 'sphingolipid metabolism' pathways were correlated with the development of DIO. Moreover, we validated that the pRb protein, key regulator of 'cell cycle pathway', was inactivated by phosphorylation in POMC neurons with HFD feeding. Importantly, reversal of deregulated cell cycle by stereotaxic delivering of the unphosphorylated pRbΔP in ARC significantly meliorated the DIO. Together, our study provides insights into the mechanisms related to the loss of homeostasis of POMC neurons in DIO, and suggests pRb phosphorylation as a potential intervention target to treat DIO.

Conclusion: The Arcuate nucleus is the material basis that controlled energy balance and glucose metabolism, which is vulnerable to high-fat-diet (HFD) in diet-induced-obesity (DIO). In this study, we conducted transcriptomic profiling in anorexigenic POMC neurons of ARC with HFD to disclose the underlying mechanisms related with the homeostasis maintenance and the development of DIO. Importantly, we suggest that DIO could be prevented of treated by reversal of the deregulated cell cycle in POMC neurons through targeting pRb phosphorylation.

Keywords: High-Fat-Diet (HFD); Diet-Induced Obesity (DIO); POMC neuron; Neuron homeostasis; pRb phosphorylation

Background

Obesity has become a worldwide pandemic issue. More than one out of eight global population showed obesity, defined as the body mass index (BMI) ≥ 30 kg/m^2 [1]. The morbid obesity is caused by a variety of environmental and genetic factors, among which the dysregulation of energy-regulating neurons followed by disorder of feeding behaviour control is fundamentally relevant. The Arcuate nucleus (ARC) in hypothalamus contains the anorexigenic POMC neurons and the orexigenic AgRP/NPY neurons for maintaining energy balance [2]. Leptin secreted by adipose tissue inhibits AgRP neurons and activates POMC neurons to exert its anorexigenic effect. However, naturally happened diet-induced obesity (DIO) is counter-intuitively associated with elevated levels of leptin, which is termed leptin resistance. Recent studies provided insights into the potential mechanisms of leptin resistance in DIO. One study showed that HFD might alter the leptin signaling transduction [3]. Other studies attributed the development leptin resistance to the loss of neurons homeostasis in ARC. For examples, Musberg revealed that HFD caused injuries to ARC neurons [4]. Besides, increased apoptosis of ARC neurons was reported in response to HFD [3, 5]. Approximately 25% loss of POMC neurons was observed after 8 months of HFD [6]. These studies suggest that detrimental effects of HFD might affect the neuron homeostasis (maintenance of the post-mitotic state, apoptosis, and survival) of ARC neurons, especially POMC neurons, to induce leptin resistance and DIO.

Several studies have proved the relationship between alteration in POMC neurons and obesity, respectively. For example, dexamethasone treatment induced increased adiposity and obesity through abrogation of glucocorticoid-regulated kinase 1 (SGK1) in POMC neurons [7]. Another study suggested that glucose sensing pathway in POMC neurons is impaired in obese mice, resulted in dysregulated glucose metabolism [8]. We previously reported that genetic mutation of *Rb1* gene significantly compromise the homeostasis of POMC neurons, but spare the co-residing AgRP neurons, leading to to a hyperphagia-obesity-diabetes syndrome in mice [9]. Despite of these individual reports, comprehensive analysis of alterations in POMC neurons with HFD is needed for understanding of how POMC neurons lose homeostasis and develop the DIO.

RNA-seq provide us with an approach for comprehensive transcriptome analysis in DIO. For examples, other groups employed RNA-seq to analyze the transcriptomic alteration in brown adipose tissue [10], brain and lung [11] of mice with HFD feeding to study how distant organ/tissue contributes to DIO. On the other hand, other groups enabled transcriptomic analysis in specific neuron subpopulation by genetics-based conditional labeling and cell sorting technique [12, 13]. Henry Sugino et al. reported the transcriptomic alteration in POMC neurons in response to food deprivation

in mice [14]. Thus, it would be interesting to employ RNA-seq to comprehensively analyze the transcriptomic variation of POMC neurons in mice with HFD feeding.

In the present study, we investigate the transcriptomic alteration of hypothalamic POMC neurons of mice with HFD. As a result, a total of 1,066 differentially expressed genes (DEGs) were identified with HFD feeding. Further bioinformatics analysis with the identified DEGs suggests that deregulation of 'sphingolipid metabolism' and 'chemokine signaling' mediated hypothalamic inflammation would induce 'cell cycle' deregulation of POMC neurons, followed by 'apoptosis'. Finally, we showed that recovery of the normal cell cycle regulation in POMC neurons by stereotaxic delivering the un-phosphorylated pRbΔP to ARC significantly meliorated the DIO in mice. Our results shed light on the underlying mechanisms as well as potential treating strategies for DIO.

Results

HFD induced obese phenotype in *Pomc*-Cre; *ROSA*-tdTomato male mice

To investigate the transcriptomic alteration of POMC neurons upon HFD feeding, we start to establish a diet-induced-obesity (DIO) mouse model. Thirty 7-weeks-old *Pomc*-Cre; *ROSA*-tdTomato male mice were randomly divided into RD groups and HFD group, and were fed with regular chow or high-fat diet for 8 weeks respectively. As shown in Fig.1A, at the initial feeding period (Day 0-15), HFD group exhibited higher caloric overconsumption relative to the RD group ($p < 0.05$), while the difference becomes negligible at the middle feeding period (Day 16-50). Interestingly, the calories intake in HFD group elevated again and becomes significantly higher than that of RD group at the final feeding period (Day 60-75), indicating that HFD feeding induced hyperphagia in our model mice. As a result, the mice of the HFD group develop severe obese phenotype, they showed significant increase of body weight and fat mass as compared to that of RD group (Fig.1B-C). At the endpoint of HFD feeding, the mice body weight of HFD group was around 40% higher than that of the RD group, and the mice abdominal white fat content in HFD group also significantly increased. The abdominal white fat of RD group and HFD group mice were shown in Fig.1D. Based on the quantification, there is significant increase of fat mass in HFD mice (Fig.1E). Together, these data indicated that HFD treatment induced a hyperphagia-obesity syndrome in *Pomc*-Cre; *ROSA*-tdTomato male mice and the DIO mouse model was well established [19, 20].

Cell sorting and RT-qPCR verification of POMC neurons

The basal hypothalamus tissue for each mice was dissected out and combined within each parallel set. As a result, three parallel biological replicates were obtained for both RD and HFD groups. In preliminary setups, we confirmed that POMC-Cre specifically turn on the tdTomato fluorescence in hypothalamic neurons in *Pomc-Cre*+;ROSA$^{-tdTomato}$ mice, while no background signal was observed in

Pomc-Cre-;ROSA$^{-tdTomato}$ mice without Cre expression (Fig.S1A). Conditional knockout of Rb1 gene will induce POMC neuron loss [9], we employed this model to further validate that, both native tdTomato fluorescence and POMC IHC staining comes up with similar POMC neuron loss rate following Rb1 conditional knockout (Fig.S1B). Thus, we are confident that tdTomato protein was specifically expressed in POMC neurons of *Pomc-Cre*+;ROSA$^{-tdTomato}$ mice. As compared to negative control samples from mice without Cre expression, we observed a specific tdTomato+ cell population (3.21%) in *Pomc-Cre*+;ROSA$^{-tdTomato}$ mice (Fig.1F & 1G). We then use the tdTomato fluorescence as a sorting marker (Ex:554,Em:581) to sort out tdTomato+ POMC neurons from RD and HFD samples. To further validate the expression of tdTomato and *Pomc* genes in sorted tdTomato+ cells, we employed qRT-PCR to analyze the gene enrichment fold in tdTomato+ cells (from P3 gating in Fig.1G) as compared to the overall non-sorted cells (from P1 gating in Fig.1G). As shown in Fig.1H, we observe the *Pomc* and tdTomato gene enriched for 67 and 110 folds respectively in sorted cells, indicating that the hypothalamic POMC neurons in both RD group and HFD groups were collected successfully.

RNA-seq data procession and DEGs identification

The sorted POMC neurons from RD and HFD groups were then subjected to transcriptome library construction and RNA-seq analysis. The Raw Data was validated by quality control (QC). The occupation of QC30 reads (mismatch rate < 0.01%) of all samples were higher than 90%, indicative of the high quality of our sequencing results. Then, low-quality reads and bases were removed from Raw Reads to generate the clean reads, which were further mapped to the mouse reference sequence (ftp://ftp.ncbi.nih. gov/refseq/M_musculus/mRNA). The quality of sequence data of all samples was listed in Table 1. These results suggested that all constructed libraries were well constructed and qualified for further analysis. We estimated the gene expression of hypothalamic POMC neurons in HFD group and RD group mice by fragments per kilobase of exon per million fragments mapped (FPKM), and differential expression genes (DEGs) by DESeq2 (listed in Supplementary file 1). Based on threshold of q-value <0.05, |Log2 fold change (FC)| > 1, a total of 1,066 genes (628 genes up-regulated and 438 genes down-regulated) were identified as differentially expressed with HFD feeding (Fig.2A). The clustering map of DEGs showed the difference of transcriptomic profile between the HFD and the RD groups, which is of statistical significance, suggesting that HFD feeding induces a transcriptomic alteration in the POMC neurons (Fig.2B&2C).

The biological function module and signaling pathways alteration in POMC neuron of HFD mice

Gene Ontology (GO) annotations have been widely used to describe attributes of genes and their classification in genome-scale analysis [21]. In the present study, a total of 1066 HFD-induced DEGs were classified based on ‘cellular component’, ‘molecular function’ and ‘biological process’ main

categories in GO database. Based on enriched gene number (FDR≤0.05), top enriched GO terms belonging to the 3 main categories respectively are shown in Fig.3A, such as 'membrane part' (120 DEGs), 'intrinsic component of membrane' (97 DEGs), 'protein binding' (167 DEGs), 'regulation of biological process' (163 DEGs) and 'regulation of cellular process' (155 DEGs). Moreover, HFD-induced DEGs are also found to be enriched in 'signal transduction', 'hydrolase activity' and 'regulation of response to stimulus' terms abundantly (Fig.3A and Supplementary file 2).

Then we applied the Fisher Exact Test to filter out the significantly changed gene list. These DEGs were applied in more specific GO enrichment analysis in 'biological process', 'cellular components', and 'molecular function' (Fig.3B-D). 'Biological process term' is described by their outcome or ending state [22]. Within the 'biological process' category, we found that the DEGs were more enriched in regulation of signalling (FDR= $5.343E^{-11}$), regulation of cell communication (FDR= $1.21E^{-12}$) and ensheathment of neurons (FDR= $5.11E^{-11}$) GO terms. The 'cellular component' category describes the subcellular structures, organelle and macromolecular complexes including a lot of cellular related enzymes and protein complexes [23]. Specifically, we found that, within 'cellular component' category, the HFD induced DEGs were more enriched in cell projection (FDR=$4.71E^{-17}$), neuron part (FDR=$1.69E^{-15}$), membrane part (FDR=$1.75E^{-14}$) and axon (FDR=$3.48E^{-10}$) GO terms. On the other hand, for 'the molecular function' category, the DEGs were more enriched in protein binding (FDR=$1.84E^{-16}$), phospholipid binding (FDR= $2.74E^{-4}$) and fatty acid elongase activity (FDR=$1.27E^{-5}$) GO terms. Collectively, these top enriched GO terms were largely related with neuron homeostasis (developmental process, regulation of apoptotic process, regulation of cell death, regulation of cell proliferation), extracellular component (cell chemotaxis, cytokine-mediated signaling, regulation of chemotaxis, chemokine-mediated signaling) and neuron metabolism (sphingolipid metabolic process, fatty acid synthase activity, cellular lipid metabolic process).

Kyoto Encyclopedia of Genes and Genomes database (KEGG) was applied for the systematically understanding of cellular functions in terms of the gene networks/pathways [24]. Genes and products cooperated in pathways to achieve their biological functions. Based on KEGG pathway analysis, several biofunction and signalling pathways were found to be altered with HFD feeding in POMC neurons (listed in Supplementary file 2). As shown in Fig.3E, 12 pathways were found to be significantly related with HFD treatment (q-value < 0.05). We observed that those top enriched KEGG pathways could be classified into 'the extracellular response' category (Leukocyte transendothelial migration, Cell adhesion molecules, Cytokine-cytokine receptor interaction, Chemokine signaling pathway) and 'metabolism regulation' category (Fatty acid metabolism, Biosynthesis of unsaturated fatty acids, Fatty acid elongation and Sphingolipid metabolism). The most significant related pathways were 'Fatty acid metabolism', indicative of the transcriptomic adaptation of POMC neurons under the HFD induced micro-environment. Moreover, the 'MAPK pathway' (q-

value= 0.0257), which is pivotal for maintaining cellular homeostasis, was also enriched for significant alteration in the HFD treated group.

GSEA functional analysis of the identified HFD-induced DEGs and RT-qPCR validation

We next performed gene-set enrichment analysis (GSEA) of the transcriptomic profiles of RD and HFD samples with the published gene sets from the Molecular Signatures Database (MSigDB 7.0) [25]. The MSigDB is composed of 165 published gene sets, each of which summarizes and defines a classical biological process. GSEA based on MSigDB 7.0 was applied to identify gene signature sets, as well as their related pathways, were enriched in our HFD feeding treatment (listed in Supplementary file 2). Base on the results, 8 gene sets (biological pathways) among them were identified to be significantly enriched in hypothalamic POMC neurons following HFD treatment ($p<0.05$), listed as follow: adipocytokine signalling (NES= -0.4), apoptosis (NES= -0.75), cell cycle (NES= 1.15), cytokine-cytokine receptor interaction (NES= -1), chemokine signalling (NES= -1.29), B-cell receptor signalling (NES= -0.96), and sphingolipid metabolism (NES= -1.3) (details listed in Table 2).

Long-term HFD induced hypothalamic inflammation might result in neuron apoptosis and cell cycle arrest [4]. Another study also suggested the correlation between hypothalamic inflammation and obesity phenotype [26]. In the present study, based on the result of GSEA analysis, we found that the HFD induced-DEGs were more enriched in the ‘cell cycle’, ‘apoptosis’, ‘chemokine signaling’ and ‘sphingolipid metabolism’ gene signatures (Fig.4A-D), suggesting that the dysregulation of lipid metabolism in HFD mice might change the microenvironment of their hypothalamus and induce chemotaxis of microglia cell to induce neuron inflammation. According to other reports, the hypothalamic inflammation would further lead to cell cycle re-entry and apoptosis of POMC neuron [27]. Thus, we focused on the specific genes among these four gene sets (Fig.S2), and compared their expression level between RD and HFD groups (Fig.4E-H). As shown in Fig.4E, the ‘DNA replication and cell cycle’ related hallmark genes such as E2F2, Mycn, Dck, Mdm4, Ptpn6 and Top2A were found to be upregulated in HFD group with the RNA-seq data. These results were further validated by RT-qPCR (Fig.4I). For the apoptosis gene set, Il1rap and Tmbim1 were validated by RT-qPCR (Fig.4F, J). Moreover, the specific genes from the ‘chemokine signaling’ and ‘sphingolipid metabolism’ including Adipor2, Vav1, Dock2, Ccr6, Olig1, Elov1, Map7, Serinc1, Serinc5 and Pla1a were validated, respectively (Fig.4G-H, K-L). Overall, the RT-qPCR validation results were in accordance with the RNA-seq data for the verified hallmark genes form 4 GESA gene signatures.

Reversal of deregulated cell cycle in POMC neurons meliorate the diet induced obesity

Among the identified four important pathways altered by HFD feeding in POMC neurons (Fig.4), ‘cell cycle regulation and E2F targets’ pathway is fundamentally correlated with the homeostasis of POMC neurons. It draws our attention that multiple targets of cell cycle related genes and E2F

associated genes were deregulated in POMC neurons with HFD feeding, leading to the exit of post-mitotic state of POMC neurons, followed by apoptotic neuron loss. Thus it would be interesting to verify in vivo whether POMC neurons are undergoing cell cycle deregulation with HFD feeding. Since pRb is the key regulator of E2F pathway and cell cycle, which is hyper-phosphorylated by CDKs[28] or AMPK[29] to permit cell proliferation. We further employed immuno-staining to check the phosphorylation of pRb(S608) in ARC POMC neurons. As shown in Fig.5A, phosphorylation of pRb(S608) could hardly be detected in RD group mice. However, following 8 weeks of HFD feeding, elevated phosphorylation of pRb(S608) is observed in about one third of POMC neurons. In contrast, phosphorylation of pRb(S608) can not be detected in astrocytes of the identical mice in HFD group (Fig. S3).

The elevated phosphorylation of pRb(S608) suggests that the POMC neuron is undergoing extensive cell cycle deregulation, which is accordance to the transcriptomic alteration of signatures of 'E2F target genes' and 'cell cycle pathway' in RNA-seq (Fig.4 and Table.2). The next question would be whether the deregulation of cell cycle is functional important for the DIO development, and whether we could mitigate DIO by preventing cell cycle deregulation of POMC neurons with HFD feeding. As known, pRb function is inactivated by consecutive phosphorylation of the Thr and Ser in Cdk consensus sequences (Fig.5B). It was determined that the most reliable way to prevent inhibiting pRb's function by phosphorylation is to mutate at least fourteen of the fifteen Thr and Ser in Cdk consensus sequences to Ala[30, 31]. The resulting pRb, which we call un-phosphorylated pRbΔP, cannot be inhibited through phosphorylation by CDKs. We constructed lentivirus expressing GFP and pRbΔP respectively, and employed the stereotaxic injection to specifically delivered lenti-GFP and lenti- pRbΔP to the ARC area of the mice at 7 weeks old (Fig.S4 A&B). The two groups of mice were further subjected to HFD feeding for the following 8 weeks. As a result, the mice injected with lenti-pRbΔP was significantly less obese than the mice injected with lenti-GFP from the third week of HFD feeding (Fig.5C). Furthermore, the decreases in fat % can largely account for the body weight reduction of mice with pRbΔP expression in ARC (Fig.5D). On the other hand, we observed sever gliosis in ARC of HFD fed mice, indicative hypothalamic inflammation with HFD feeding (Fig.S4C). This immuno-staining result further confirmed the transcriptomic alteration of signatures of 'chemokines signaling' and 'inflammation pathway' in RNA-seq profiling (Fig.4 and Table.2). However, the hypothalamic inflammatory microenvironment was also significantly mitigated with un-phosphorylated pRbΔP expression in ARC (Fig.S4C). Collectively, these results validated that 'cell cycle deregulation' is fundamental cause of loss of homeostasis of POMC neurons and the DIO development, and suggests that we could treat DIO through recovering the cell cycle regulation of POMC neurons.

Discussion

The hypothalamus contains complex neuronal circuits for energy balance. ARC nucleus, located in the proximity to the median eminence of hypothalamus with incomplete blood-brain-barrier (BBB), is especially vulnerable to the microenvironment change. Components of the diet are amongst the most important factors that modulate hypothalamic function [32]. Studies have shown that dietary fats can promote severe damage in neurons of the medium-basal hypothalamus [33-37]. POMC neurons, but not the AgRP neurons, has been reported to be required for normal compensatory refeeding [38]. During the development of diet-induced-obesity mice model, the local inflammation triggered by dietary fats can, early on, produce hypothalamic resistance to the catabolic actions of leptin and insulin [33, 36, 39]. Although it's now more accepted that HFD could cause injuries to hypothalamic POMC neurons and leads to diet-induced-obesity, the comprehensive understanding of the underlying mechanisms during this process is still needed.

Recent studies have begun to connect these two aspects by showing that HFD can cause injuries to POMC neurons through altering the transcriptional activity of STAT3 and SRC-1, the critical regulator of POMC neurons, leading to the transcriptomic alteration in POMC neurons [3, 40]. This might shed some light on the pathogenesis of DIO. RNA-seq, an approach for transcriptomic analysis, does not rely on a predesigned probe and enables rapid profiling and deep investigation of the transcriptome for any tissues or species, taking more advantages over traditional microarray analysis particularly for low abundance transcripts [39, 41, 42]. Here we constructed the HFD mice model and compared the HFD induced transcriptome alteration in POMC neuron with RNA-seq approach (Fig.1).

We employed multiple bioinformatics approaches to analyse the obtained RNA-seq data. KEGG pathways analysis indicated that the HFD significantly affects 'sphingolipid metabolism' pathways, 'cell cycle regulation', 'fatty acid metabolism' pathways and the 'exocellular and inflammation'. The 'Gene Ontology' analysis indicated that the HFD induced DEGs in POMC neurons mostly enriched in the 'neuron development', 'neuron ensheathment process' and 'regulation of signal transduction process'. From the GSEA results, the top enriched gene signatures were 'sphingolipid metabolism' 'cell cycle', 'apoptosis', 'chemokine signalling' pathways' and 'B-cell receptor signalling'. Collectively, the transcriptomic profiling indicated that HFD might firstly affect the 'sphingolipid metabolism' pathway to cause dysregulation of neuron development and then activate 'chemokine signaling' to induce local inflammation, both of which further leads to deregulation of "cell cycle and E2F targets' pathway. Aberrant cell cycle re-entry leads to activation of 'apoptosis pathway' to induce neuron loss of POMC neurons. Eventually, the POMC neurons lose homeostasis and develop DIO.

The Sphingolipid Metabolism Pathway

Sphingolipids, in particular ceramide, were first identified in the brain more than a century ago [43]. Sphingolipids have been reported to regulate apoptosis, survival and differentiation of neurons [44].

For examples, myelin defects would result in axon degeneration and contributes to the pathogenesis of demyelinating diseases [45]. The sphingolipid metabolism pathway is also involved in the TNF induced apoptotic neuron loss [46]. In the present study, genes of 'sphingolipid metabolism pathway', including *Asah2*, *Cers2* and *Elovl1* were identified to be upregulated in POMC neurons in HFD group mice (Fig.4H&L). Upregulation of sphingolipid metabolism factor, e.g., Asah2, could promote mitosis and apoptosis through increasing sphingosine production[47]. Cers2 and Elovl1 are also reported to mediate cell growth and cerebral degeneration[48, 49]. Presumably, the deregulation of 'Sphingolipid Metabolism Pathway' in might be involved with the loss of homeostasis of POMC neurons under HFD feeding condition.

Chemokine Signalling Pathways

The abundant by-product of lipid metabolism might cross the median eminence, a location with incomplete blood-brain-barrier (BBB), to change the microenvironment of ARC area of HFD group mice. As reported, the neurons, under abnormal pathological conditions, were able to release chemokines to provide directional cues for the cell trafficking, including immune cells [50]. These chemokines mediated local inflammation is important for self-protective host response, but is also possible to be related with the loss of homeostasis of neurons under certain conditions. Moreover, deregulation of 'sphingolipid metabolism pathway' might also change the microenvironment in ARC and induce inflammation[49]. Consistent to this scenario, several genes belonging to 'chemokine signalling' were found to be upregulated in POMC neurons with HFD feeding (Fig.4G&K). For example, Tyrosine kinase binding protein gene (*Tyrobp*), which is reported to mediate chemokine signalling transduction and inflammation [51, 52], upregulated about 15 folds in POMC neurons of HFD fed mice as compared to the RD group mice. The *Bmp2 and Bmp7*, which function in hypothalamic neural fate decision [53], were found to increase their expression in POMC neurons with HFD feeding. Moreover, the C-C chemokine receptor type 6 gene (*Ccr6*) also upregulated significantly in POMC neurons in response to HFD feeding in the present study. These results, together with the literatures, suggests that'chemokine signaling'is activated in POMC neurons to recruit immune cells, e.g., brain microphage microglia cells, to induce local inflammation in ARC with HFD.

Cell Cycle Pathway

The differentiated neurons are maintained in post-mitotic state, which is typically different from other cell types. However, the expression of a number of cell cycle genes including cyclin D1, Cdk4, and E2Fs were detected in different quiescent state in the adult nervous system [54]. Thus, the cell cycle re-entry of differentiated neurons remained possible under certain pathological conditions such as neurotrophic factor deprivation, oxidative stress and excitotoxicity [55]. In this regard, E2F1 can trigger the neuron apoptosis following aberrant cell cycle re-entry [56, 57]. In present study, we found

that several genes belonging to 'cell cycle regulation and E2F targets' pathway show significant alteration in POMC neurons after 8 weeks of HFD feeding. For examples, 'cell cycle checkpoint' genes such as *Cdkn1c* were found to be downregulated, while genes related to DNA replications and G1/S transition, such as *Mdm4*, *Ptp4a1*[58] and *Prim1a*, showed significant upregulation in POMC neurons of HFD group mice (Fig.4E&I). These data indicate that HFD induces cell cycle deregulation in POMC neurons, which is in accordance with the immunostaining data that pRb protein, the key regulator of cell cycle, was inhibited by phosphorylation at Serine608 in about one third of POMC neurons with HFD feeding (Fig.5A). Importantly, overexpression of un-phosphorylated pRb mutant in ARC significantly meliorated the obese phenotype caused by HFD feeding (Fig. 5C&D). These data demonstrate that 'cell cycle regulation' pathway is fundamentally important for the homeostasis maintenance of POMC neurons, which is compromised by HFD to induce obese phenotype.

Apoptosis Pathway

Apoptosis is a programmed biological process to eliminate damaged or redundant cells. In differentiated neurons, aberrant cell cycle re-entry is usually followed by apoptosis and neuron loss [59, 60]. HFD could cause neuron injury and inflammation [61]. Would these further lead to apoptosis of POMC neurons? We showed in our results that, Bcl2l11, an anti-apoptotic member of the BCL2 family, was downregulated in POMC neurons with HFD feeding. In contrast, pro-apoptotic genes, such as the tumour necrosis factor (*Tnf*), transmembrane BAX Inhibitor Motif Containing 1 (*Tmbim1*) and cathepsin S (*Ctss*), upregulated in POMC neurons of HFD mice (Fig.4F&J). Thus, POMC neurons were indeed undergoing apoptotic neuron loss with HFD feeding, accounting for the occurrence of leptin resistance and diet induced obesity.

Taken together, we propose a schematic model to illustrate the mechanisms that leads to loss of homeostasis of POMC neurons with HFD feeding in DIO mice model (Fig. 5E). Firstly, long-term HFD induces deregulation of sphingolipid metabolism pathway. The accumulation of sphingolipid and ceramide would further initiate inflammasome formation and activation and alter the hypothalamic microenvironment, where POMC neurons located[47]. Besides, the chemokine signalling activated in POMC neurons of DIO mice to recruit versatile immune cells, e.g., microglia cells [62]. Following these alteration, pRb protein is inactivated by phosphorylation (Fig. 5A) to permit the deregulation of E2Fs transcriptional activity, which results in aberrant cell cycle re-entry and apoptosis in POMC neurons. Eventually, the homeostasis of POMC neuron was compromised, leading to DIO in mice. Based on the hypothesized model, we suggest that DIO could be prevented or treated by reversal of the deregulated cell cycle in POMC neurons through targeting pRb phosphorylation.

Conclusion

The present study is the first report to analyze the transcriptomic alteration of anorexigenic POMC neurons of ARC following HFD feeding. The results revealed that 'cell cycle', 'apoptosis', 'chemokine signalling' and 'sphingolipid metabolism' pathways were implicated with loss of homeostasis of POMC neurons in DIO mice. The deregulation of 'sphingolipid metabolism' and activation 'chemokine signalling' would induce hypothalamic microinflammation, leading to aberrant cell cycle re-entry and apoptosis of POMC neurons in HFD fed mice. We further validated that HFD feeding induced inhibitive phosphorylation of pRb, which is the key regulator of cell cycle regulation. Moreover, by functional rescue of pRb in ARC significantly meliorated the DIO. Together, our study provides insights into the mechanisms related to the loss of homeostasis of POMC neurons in DIO, and suggests pRb phosphorylation as a potential intervention target to treat DIO.

Methods and materials

Animals and genotyping

All the experimental protocols were approved by Fuzhou University Animal Care Committee, conforming to accepted standards of humane animal care (Approval ID: 2019-SG-022). *Pomc*-Cre mice (Stock No. 005965) *ROSA*-tdTomato mice (Stock No. 007676) were purchased from Jackson Laboratory respectively and crossed to generate *Pomc*-Cre; *ROSA*-tdTomato offsprings for this study. The offspring were tail biopsied and genotyped at postnatal day 12 using established PCR protocols. Genotyping primers are listed in Supplementary file 1. All mice were housed in a specific pathogen–free facility with a 12 h light-dark cycle.

Establishment of HFD mice model

Male Pomc-Cre; ROSA-tdTomato mice generated for this study were on C57BL/6J x129Sv strain background. All mice were fed with standard chow (Research Diets, D12450J, 3.85 kcal/g, 10% fat, 20% protein, 70% carbohydrates) till 7-week-old. Then we selected 30 mice of similar body weight (around 20 g) and divided them into regular diet (RD) and high-fat diet (HFD) groups. Both RD and HFD groups contain 3 parallel sets, with 5 mice of each set (n=5x3). Mice in the HFD group received ad libitum access to a nutritionally complete high-fat diet (Research Diets, D-12492, 5.24 kcal/g, 60% fat, 20% protein, 20% carbohydrates) in the experiment for 8 weeks. On the same period of time, mice of the RD group were maintained on standard chow. We weighed the food consumption for RD and HFD groups mice every day throughout the experiment to compare the food intake difference. The body weight was measured every week throughout the experiment. Mice in the RD group and in

the HFD group were sacrificed by cervical dislocation at the end of experiment. The abdominal white fat of each mouse was collected and measured.

Isolated hypothalamic POMC neurons using fluorescence-activated cell sorting (FACS)

We dissected out the basal hypothalamus for individual mouse of RD and HFD groups. Together, 3 parallel biological replicates, each containing 5 basal hypothalamus from littermates, for both RD and HFD groups were finally obtained. We further minced the hypothalamus tissues, and separated out individual neurons with Papain dissociation system kit (Worthington). The neuronal cell suspension was then filtered through a 70 μm cell strainer into a new 5 mL Falcon tube for cell sorting. The aggregated cells and fractured cells were first gated out according to cell size (FSC), cell granularity (SSC). Further, with the tdTomato fluorescence as a sorting marker (Ex:554,Em:581), tdTomato+ POMC neurons of each sample from the RD and the HFD groups were sorted out. Target neurons were collected into a 96 well plate containing lysis buffer with RNase inhibitor.

RNA-seq

The RNA-seq was performed by Annoroad Gene Technology (Beijing) Co., Ltd. The sorted POMC neuron of HFD and RD mice were sent to the Annoroad Gene Technology (Beijing). The samples were prepared and the cDNA libraries were generated by using the Smart-seq2 protocol [15]. Briefly, Total mRNA was extracted by a Dynabeads mRNA DIRECT TM Kit (Ambion by Life Tech). Then the cDNA library was constructed using NEBNext Ultra TM Directional RNA Library Prep Kit for Illumina (New England BioLabs Inc.). After fragmentation and conjugation with sequencing adapters, the cDNA libraries were sequenced on Illumina Hiseq 2500 platform using PE100 strategy. The raw data from RNA-seq were filtered and mapped to reference genome (Mus_musculus.GRCm38.90.chr) by using FASTX. The FPKM (fragments per kilobase of exon model per million reads mapped) was calculated from the filtered and mapped clean Raw Reads. Then we employed the tximport package with default parameters to remove abnormal low-/high-abundance transcripts from transcriptomic profiles. Finally, the DEGs was obtained from DESeq2 analysis and used for further bioinformatic study.

Bioinformatics analysis

The sequencing results were processed further, the clean reads from the RNA-seq libraries were mapped to the mouse reference genome (Mus_musculus.GRCm38.90.chr) with HISAT2 v2.1.0. Differential expression analysis of six samples was performed using the DESeq2. We identified differentially expressed genes (DEGs) was based on the criteria that $P < 0.05$ and $|\log2(\text{fold change})| > 1$. The P-values were adjusted using the Benjamini and Hochberg method. The volcano plot of DEGs and cluster diagrams were made by R packages “ggplots” and “ggplot2,” respectively. The Gene ontology (GO) analysis includes three domains, there are molecular function, cellular component and biological process. The GO analysis was performed to predict the function of DEGs [16]. KEGG

pathway was based on the Kyoto Encyclopedia of Genes and Genomes database, and it was performed to explore the pathways related to these DEGs [17]. A p value of less than 0.05 was considered statistically significant. Gene Set Enrichment Analysis (GSEA) algorithm was used to analyze the genes/pathways genes associated with HFD [18]. Co-expression gene networks for cell-cycle pathway, apoptosis pathway, chemokine signaling pathway, and sphingolipid pathways were constructed from the normalized DEGs by Morpheus (https://software.broadinstitute. org/morpheus/) with Hierarchical Clustering. The enrichment ratio of these pathways was ranked based on the normalized enrich scores (NES). The coefficient r in each gene set was calculated by the Pearson correlation.

qPCR validation

To characterize the expression alteration of transcripts affected by HFD, we performed RT–PCR using a list of specific genes in cell-cycle pathway, apoptosis pathway, chemokine signalling pathway, and sphingolipid pathways to validate the robustness of the module analysis. RNA was extracted out from basal hypothalamus tissues from RD and HFD cohorts respectively and reversed transcribed to cDNA with cDNA Synthesis Kit (Thermo Scientific, K1622) according to the manufacture's protocol. RT-qPCR was performed using iTaq Universal SYBR Green Supermix (Bio-rad, 172-5121). The mRNA levels of target genes were normalized to GAPDH. The RT-qPCR primers for these DEGs are listed in Supplementary file 3.

Brain preparation and Immunohistochemistry

The brain of mice were dissected out and post-fixed in 4% PFA for 12 h (O/N) in 4℃ and cryoprotected with 30% sucrose for 48 h. Tissues were embedded in OCT gel (Tissue Tek), 20 mm thick coronal sections were collected on Superfrost Plus slides. Sections were first treated with 3% H_2O_2 to quench endogenous peroxidase, and subjected to blocking in 10% normal goat serum followed by antibody incubation. Finally, color development was performed using DAB Immunohistochemistry Color Development Kit (Sangon Biotech, E670033). Primary antibodies are listed: abbit phospho-Rb (Ser608) was from Cell Signaling, Rabbit polyclonal antibody against porcine POMC (27-52) was from Phoenix Pharmaceuticals

Stereotaxic injection

Un-phosphorylated pRb (pRbΔP) lentivirus was produced by co-transfecting 293T cells with the lenti-CMV-pRbΔP plasmid, the viral packaging plasmid dvpr and the viral envelope gene Vsvg. Mice were anesthetized and placed in a stereotaxic frame. We stereotaxically injected viruses of lenti-CMV-pRbΔP and lenti-CMV-GFP (1.5 μL, 4×10^7 PFU/mL) into mice at the hypothalamus (Milli meter from bregma: + 1.46 antero-posterios, + 0.8 medio-lateral, - 5.8 dorso-ventral) using Microinjection springer pump (GenieTouch™ Syringe Pump, Kent Scientific) with the speed of 0.4 μL/min.

Statistical analysis

Statistical analyses were performed using GraphPad Prism 6. Significant differences were calculated using an unpaired *t* test and the Pearson correlation. All results were expressed as the mean ± standard deviation. A $p < 0.05$ was considered statistically significant.

Abbreviations

ARC	Arcuate nucleus
DEGs	differentially expressed genes
DIO	Diet-Induced Obesity
GO	Gene Ontology
GSEA	gene-setenrichment analysis
HFD	High-Fat-Diet
HFD	high fat diet
KEGG	Kyoto Encyclopedia of Genes and Genomes database
MAPK	mitogen-activated protein kinase
MBH	Medialbasal hypothalamus
PPI	protein-prote ininteraction
RD	regular diet
VMN	Ventromedial nucleus

Declarations

Ethics approval and consent to participate

All the experimental protocols in this study were approved by Fuzhou University Animal Care Committee, conforming to accepted standards of humane animal care (Approval ID: 2019-SG-022).

Consent for publication

Not Applicable

Competing interests

The authors confirm that there is no conflict of interest.

Availability of data and materials

All data generated or analysed during this study are included in this published article and its supplementary information files.

Funding

This study was supported by the National Natural Science Foundation of China (Nos. 81600662，81772759), the National Natural Science Foundation of Fujian Province (No. 2019J01240) and the Talent Foundation of Fuzhou University (No. XRC-1625) to Professor Zhonglei Lu's research group. The funding bodies provided financial assistance to support this study only. As such, neither funder was involved in the study design, data collection, analysis or interpretation, or in manuscript preparation.

Authors' contributions

P.L., ZS.H., QJ.F., analysed and interpreted the experimental data and RNA-seq data generated in this study. YF.S., MY.Z., YN.H., and X.C. performed the molecular biology experiments. analysed the results of the molecular biology experiments. P.L., ZL.L. performed the histological and immunohistochemistry examination of the hypothalamic, and was a major contributor in writing the manuscript. All authors read and approved the final manuscript.

Acknowledgement

Not Applicable

References

1. Nordang, G.B., et al., *Next-generation sequencing of the monogenic obesity genes LEP, LEPR, MC4R, PCSK1 and POMC in a Norwegian cohort of patients with morbid obesity and normal weight controls.* Molecular genetics and metabolism, 2017. **121**(1): p. 51-56.
2. Schwartz, M.W., et al., *Central nervous system control of food intake.* Nature, 2000. **404**(6778): p. 661.
3. Münzberg, H., J.S. Flier, and C. Bjørbæk, *Region-specific leptin resistance within the hypothalamus of diet-induced obese mice.* Endocrinology, 2004. **145**(11): p. 4880-4889.
4. Münzberg, H. and M.G. Myers Jr, *Molecular and anatomical determinants of central leptin resistance.* Nature neuroscience, 2005. **8**(5): p. 566.
5. Moraes, J.C., et al., *High-fat diet induces apoptosis of hypothalamic neurons.* PloS one, 2009. **4**(4): p. e5045.
6. Thaler, J.P., et al., *Obesity is associated with hypothalamic injury in rodents and humans.* The Journal of clinical investigation, 2012. **122**(1): p. 153-162.
7. Deng, Y., et al., *SGK1/FOXO3 Signaling in Hypothalamic POMC Neurons Mediates Glucocorticoid-Increased Adiposity.* Diabetes, 2018. **67**(4): p. 569-580.
8. Parton, L.E., et al., *Glucose sensing by POMC neurons regulates glucose homeostasis and is impaired in obesity.* Nature, 2007. **449**(7159): p. 228.
9. Lu, Z., et al., *pRb is an obesity suppressor in hypothalamus and high-fat diet inhibits pRb in this location.* The EMBO journal, 2013. **32**(6): p. 844-857.
10. Cao, J., et al., *Global transcriptome analysis of brown adipose tissue of diet-induced obese mice.* International journal of molecular sciences, 2018. **19**(4): p. 1095.
11. Xiao, Y., et al., *The effects of short-term high-fat feeding on exercise capacity: multi-tissue transcriptome changes by RNA sequencing analysis.* Lipids in health and disease, 2017. **16**(1): p. 28.
12. Okaty, B.W., K. Sugino, and S.B. Nelson, *A quantitative comparison of cell-type-specific microarray gene expression profiling methods in the mouse brain.* PloS one, 2011. **6**(1): p. e16493.
13. Sugino, K., et al., *Molecular taxonomy of major neuronal classes in the adult mouse forebrain.* Nature neuroscience, 2006. **9**(1): p. 99.
14. Henry, F.E., et al., *Cell type-specific transcriptomics of hypothalamic energy-sensing neuron responses to weight-loss.* Elife, 2015. **4**: p. e09800.
15. Picelli, S., et al., *Full-length RNA-seq from single cells using Smart-seq2.* Nature protocols, 2014. **9**(1): p. 171.
16. Consortium, G.O., *The Gene Ontology (GO) database and informatics resource.* Nucleic acids research, 2004. **32**(suppl_1): p. D258-D261.
17. Ogata, H., et al., *KEGG: Kyoto encyclopedia of genes and genomes.* Nucleic acids research, 1999. **27**(1): p. 29-34.
18. Subramanian, A., et al., *Gene set enrichment analysis: a knowledge-based approach for interpreting genome-wide expression profiles.* Proceedings of the National Academy of Sciences, 2005. **102**(43): p. 15545-15550.

19. Speakman, J., et al., *Animal models of obesity.* Obesity Reviews, 2010. **8**(s1): p. 55-61.
20. Wang, C.Y. and J.K. Liao, *A mouse model of diet-induced obesity and insulin resistance.* Methods Mol Biol, 2012. **821**(821): p. 421-433.
21. Consortium, G.O., *The Gene Ontology project in 2008.* Nucleic Acids Research, 2008. **36**(Database issue): p. D440-D444.
22. Consortium, T.G.O., *Expansion of the Gene Ontology knowledgebase and resources.* Nucleic Acids Res., 2017. **45**(D1): p. D331-d338.
23. Roncaglia, P., et al., *The Gene Ontology (GO) Cellular Component Ontology: integration with SAO (Subcellular Anatomy Ontology) and other recent developments.* J Biomed Semantics, 2013. **4**(1): p. 20.
24. Ogata, H., ., et al., *KEGG: Kyoto Encyclopedia of Genes and Genomes.* Nucleic Acids Research, 2000. **27**(1): p. 29-34.
25. Liberzon, A., *A Description of the Molecular Signatures Database (MSigDB) Web Site*. 2014.
26. Fan, W., et al., *Obesity or Overweight, a Chronic Inflammatory Status in Male Reproductive System, Leads to Mice and Human Subfertility.* Frontiers in Physiology, 2017. **8**: p. 1117.
27. Cesar, H.C. and L.P. Pisani, *Fatty-acid-mediated hypothalamic inflammation and epigenetic programming.* Journal of Nutritional Biochemistry, 2017. **42**: p. 1-5.
28. Knudsen, E.S. and J.Y. Wang, *Dual mechanisms for the inhibition of E2F binding to RB by cyclin-dependent kinase-mediated RB phosphorylation.* Mol Cell Biol, 1997. **17**(10): p. 5771-83.
29. Dasgupta, B. and J. Milbrandt, *AMP-activated protein kinase phosphorylates retinoblastoma protein to control mammalian brain development.* Dev Cell, 2009. **16**(2): p. 256-70.
30. Brown, V.D., R.A. Phillips, and B.L. Gallie, *Cumulative effect of phosphorylation of pRB on regulation of E2F activity.* Mol Cell Biol, 1999. **19**(5): p. 3246-56.
31. Chew, Y.P., et al., *pRB phosphorylation mutants reveal role of pRB in regulating S phase completion by a mechanism independent of E2F.* Oncogene, 1998. **17**(17): p. 2177-86.
32. Souza, C.T., De, et al., *Consumption of a fat-rich diet activates a proinflammatory response and induces insulin resistance in the hypothalamus.* Endocrinology, 2005. **146**(10): p. 4192-4199.
33. Marciane, M., et al., *Saturated fatty acids produce an inflammatory response predominantly through the activation of TLR4 signaling in hypothalamus: implications for the pathogenesis of obesity.* Journal of Neuroscience, 2009. **29**(2): p. 359-370.
34. Xiaoqing, Z., et al., *Hypothalamic IKKbeta/NF-kappaB and ER stress link overnutrition to energy imbalance and obesity.* Cell, 2008. **135**(1): p. 61-73.
35. Thaler, J.P., et al., *Obesity is associated with hypothalamic injury in rodents and humans.* Journal of Clinical Investigation, 2012. **122**(1): p. 153-162.
36. Moraes, J.C., et al., *High-fat diet induces apoptosis of hypothalamic neurons.* Plos One, 2009. **4**(4): p. e5045.
37. Levin, B.E. and A.A. Dunnmeynell, *Reduced central leptin sensitivity in rats with diet-induced obesity.* American Journal of Physiology Regulatory Integrative & Comparative Physiology, 2002. **283**(4): p. R941.
38. Xu, A.W., et al., *Effects of hypothalamic neurodegeneration on energy balance.* Plos Biology, 2005. **3**(12): p. e415.
39. Shanrong, Z., et al., *Comparison of RNA-Seq and microarray in transcriptome profiling of activated T cells.* Plos One, 2014. **9**(1): p. e78644.
40. Yang, Y., et al., *Steroid receptor coactivator-1 modulates the function of Pomc neurons and energy homeostasis.* Nature Communications, 2019. **10**(1): p. 1718.
41. Hoen, P.A.C., 'T, et al., *Deep sequencing-based expression analysis shows major advances in robustness, resolution and inter-lab portability over five microarray platforms.* Nucleic Acids Research, 2008. **36**(21): p. e141-e141.
42. Xinwei, H., et al., *Transcriptome of embryonic and neonatal mouse cortex by high-throughput RNA sequencing.* Proc Natl Acad Sci U S A, 2009. **106**(31): p. 12741-12746.
43. Echten-Deckert, G.V. and T. Herget, *Sphingolipid metabolism in neural cells.* Biochim Biophys Acta, 2007. **1758**(12): p. 1978-1994.

44. Chaves, E.I.P.D., *Sphingolipids in apoptosis, survival and regeneration in the nervous system.* BBA - Biomembranes, 2006. **1758**(12): p. 1995-2015.
45. Pike, L.J., *Lipid rafts: heterogeneity on the high seas.* Biochemical Journal, 2004. **378**(2): p. 281-92.
46. Sortino, M.A., et al., *Tumor necrosis factor-alpha induces apoptosis in immortalized hypothalamic neurons: involvement of ceramide-generating pathways.* Endocrinology, 1999. **140**(10): p. 4841-4849.
47. Choi, S. and A.J. Snider, *Sphingolipids in High Fat Diet and Obesity-Related Diseases.* Mediators Inflamm, 2015. **2015**: p. 520618.
48. Schnaar, R.L. and P.H. Lopez, *Myelin-associated glycoprotein and its axonal receptors.* J Neurosci Res, 2009. **87**(15): p. 3267-76.
49. Kang, S.C., et al., *Sphingolipid metabolism and obesity-induced inflammation.* Front Endocrinol (Lausanne), 2013. **4**: p. 67.
50. Haas, A.H., De, et al., *Neuronal chemokines: versatile messengers in central nervous system cell interaction.* Molecular Neurobiology, 2007. **36**(2): p. 137-151.
51. Lanier, L.L., et al., *Immunoreceptor DAP12 bearing a tyrosine-based activation motif is involved in activating NK cells.* Nature, 1998. **391**(6668): p. 703.
52. Paloneva, J., et al., *Loss-of-function mutations in TYROBP (DAP12) result in a presenile dementia with bone cysts.* Nature genetics, 2000. **25**(3): p. 357.
53. Kyoji, O., et al., *Directed differentiation of neural cells to hypothalamic dopaminergic neurons.* Development, 2005. **132**(23): p. 5185.
54. Frade, J.M. and M.C. Ovejero-Benito, *Neuronal cell cycle: the neuron itself and its circumstances.* Cell Cycle, 2015. **14**(5): p. 9.
55. Becker, E.B.E. and A. Bonni, *Cell cycle regulation of neuronal apoptosis in development and disease.* Progress in Neurobiology, 2004. **72**(1): p. 1-25.
56. Woods, J., M. Snape, and M.A. Smith, *The cell cycle hypothesis of Alzheimer's disease: Suggestions for drug development.* BBA - Molecular Basis of Disease, 2007. **1772**(4): p. 503-508.
57. Verdaguer, E., et al., *Implication of the transcription factor E2F-1 in the modulation of neuronal apoptosis.* Biomedicine & Pharmacotherapy, 2007. **61**(7): p. 390-399.
58. Werner, S.R., et al., *Enhanced cell cycle progression and down regulation of p21(Cip1/Waf1) by PRL tyrosine phosphatases.* Cancer Letters, 2003. **202**(2): p. 201-211.
59. Kruman, I.I., *Why do neurons enter the cell cycle?* Cell Cycle, 2004. **3**(6): p. 767-771.
60. Park, D.S., et al., *Involvement of retinoblastoma family members and E2F/DP complexes in the death of neurons evoked by DNA damage.* Journal of Neuroscience the Official Journal of the Society for Neuroscience, 2000. **20**(9): p. 3104-14.
61. Williams, L.M., et al., *Proteomics reveals that a high-fat diet induces rapid changes in hypothalamic proteins related to neuronal damage and inflammation.* Proceedings of the Nutrition Society.
62. Cai, D. and S. Khor, *"Hypothalamic Microinflammation" Paradigm in Aging and Metabolic Diseases.* Cell Metab, 2019. **30**(1): p. 19-35.

Figure Legends

Fig.1 The construct of DIO model of *Pomc*-Cre; *ROSA*-tdTomato mice and the cell sorting of hypothalamic POMC neurons. (A) Average (± SEM) 24 h caloric intake (kcal) of the regular diet (RD) group and the high-fat diet (HFD) group mice. (B) Body weight of the RD group and the HFD group mice. (C) Body weight gain of the RD group and the HFD group mice. (D) Abdominal white fat of the RD group and the HFD group mice. (E) The quantification of abdominal white fat of the RD group and the HFD group mice. The flow cytometric sorting of hypothalamic neurons from *Pomc-cre*-;$ROSA^{tdTomato}$ mice (F) and *Pomc-Cre*+; $ROSA^{-tdTomato}$ mice (G). (H) The enrichment of *Pomc* and tdTomato genes in sorted tdTomato+ cells (P3 of Fig.1G) as compared to non-sorted cells (P1 in Fig.1G)

Fig.2 The analysis results of differentially expressed genes. (A) Venn diagram for DEG between HFD group and RD group (Upregulated in HFD: blue, Upregulated in RD: green). Reported DEGs required q-value <0.05, abs[log2(fc)] > 1. (B) The volcano map of differentially expressed genes. NA means no significant change between HFD and RD. (C) The clustering map of differentially expressed genes. HFD indicated high fat diet group, and RD indicated regular diet group.

Fig.3 Functional analysis of differentially expressed gene (DEG) in POMC neurons of HFD group compared to RD group. (A) GO functional classification of DEGs according to the enriched gene numbers. (corrected P value < 0.05). Top enriched GO terms of 17 cellular components, 25 molecular functions and 12 biological processes were shown. (B-D) The significant pathway enrichment in GO cellular components, biological process, and molecular functions pathways according to the Bonferroni corrected False Discovery Rate (FDR) and gene counts. (E) The significant KEGG pathway enrichment. Gene counts and p-value corrected by Bonferroni are shown.

Fig.4 Pathway correlation analysis and RT-qPCR validation of differentially expressed genes (DEGs) of POMC neurons in HFD group compared to RD group. (A-D) The GSEA plots showing the enrichment of indicated gene set categories of identified DEGs. NES: normalized enrichment score. Positive NES indicates enrichment of gene signatures in HFD group, negative NES indicates enrichment of gene signatures in RD group. (E-H) The expression heatmaps and clustering of identified DEGs, classified belonging to indicated KEGG pathways. Red signal denotes higher abundance, while blue signal denotes lower abundance. (I-L) The RT-qPCR validation of selected DEGs belonging to related KEGG pathways as in plots E-H. "*", "**" and "***" indicated $p < 0.05$, $p < 0.01$ and $p < 0.001$, respectively. The representative KEGG pathways were shown: pathway of cell cycle genes and E2F targets (A, E, I), pathway of apoptosis genes (B, F, J), chemokine signal pathway (C, G, K), pathway of sphingolipid metabolism (D, H, L).

Fig.5 HFD induced phosphorylation of pRb in POMC neurons and stereotaxic injection of un-phosphorylated pRb in ARC meliorated the HFD induced DIO. (A) ARC sections from *Pomc-Cre; RosaR(GFP)* mice in RD and HFD groups were stained with pRb(S608p). Direct GFP was photographed in green. (B) Phosphorylation sites of pRb protein and the schematic maps of the lenti-GFP and lenti-pRbΔP plasmids. (C) Body weights and body weight gains of the HFD fed mice injected with lenti-GFP or lenti-pRbΔP lentivirus in ARC (n=5 for each group) . (D) Abdominal white fat content of HFD fed mice injected with lenti-GFP or lenti-pRbΔP lentivirus in ARC (n=5 for each group). (E) Predicted schematic model of HFD induced POMC neuron dysregulation.

Fig.S1 (A) ARC from the wild-type control and Pomc-Cre;$Rosa^{tdTomato}$ mice. The fluorescent marker native tdTomato was found specifically expressed in ARC POMC neurons. (B) Rb1 is required for POMC neuron maintenance. POMC neuron numbers were counted on sections. Deficiency of Rb1

resulted in approximately 65% decrease of POMC neuron and 70% decrease of tdTomato neurons, which indicated the specifically expression of tdTomato in POMC neurons.

Fig.S2 The expression level of specific genes and gene correlation landscape of (A) cell cycle pathway (B) apoptosis pathway (C) chemokine signal pathway (D) sphingolipid metabolism pathway.

Fig.S3 HFD induced pRb phosphorylation does not exist in astrocytes. ARC sections from *Pomc-Cre; RosaR(GFP)* mice in RD and HFD groups were co-stained with antibodies against pRbS608p (red) and GFAP (green).

Fig.S4. (A) The relative mRNA level of WPRE in the hypothalamus injected with lenti-GFP or lenti-pRb∆P virus. (B) Native GFP fluorescence image of ARC injected with lenti-GFP virus. (C) ARC sections from mice in RD group and HFD group injected with lenti-GFP or lenti-pRb∆P virus were co-stained with antibody against allograft inflammatory factor 1 (Iba1) and DAPI to indicate hypothalamic inflammation status

Figures

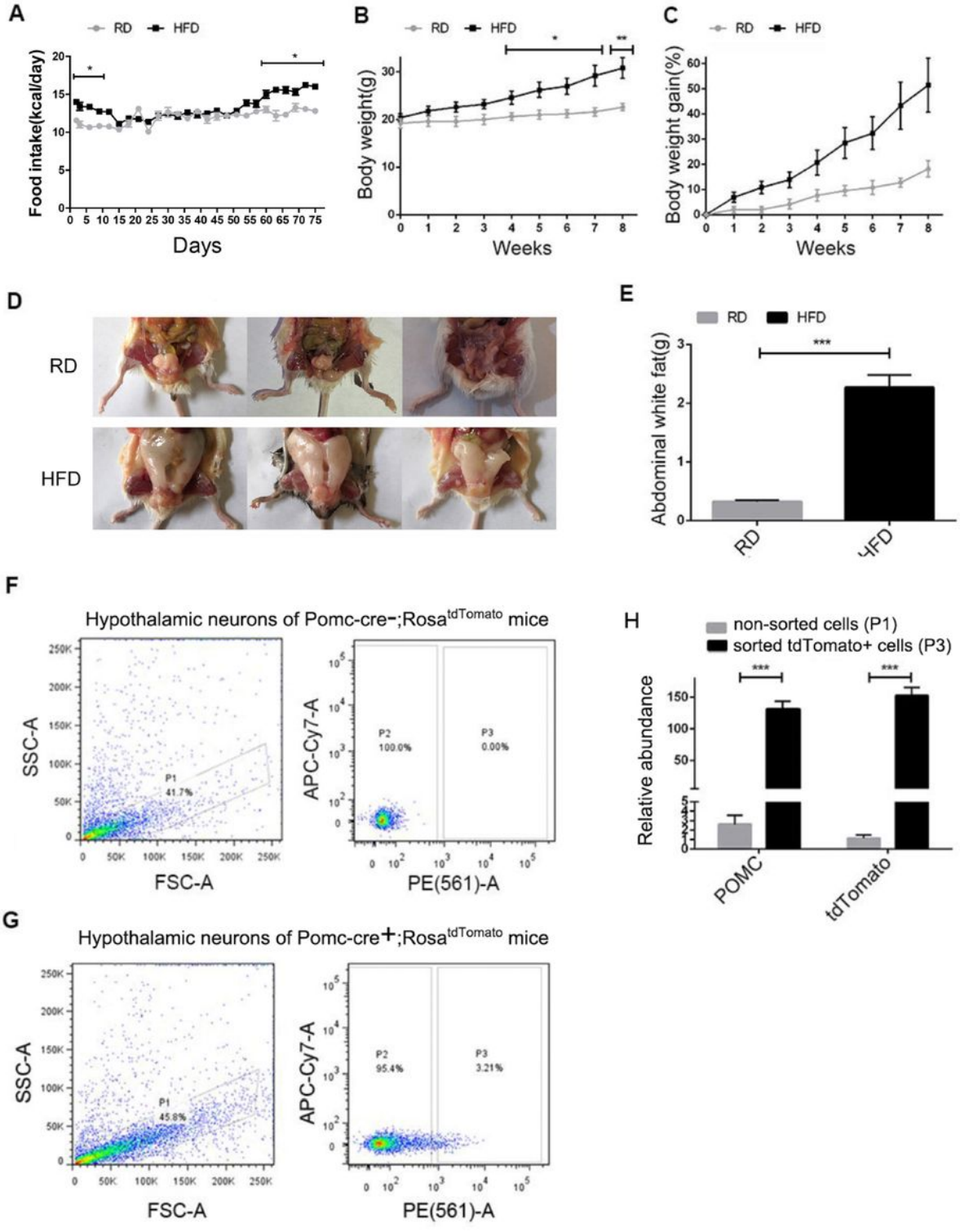

Figure 1

The construct of DIO model of Pomc-Cre; ROSA-tdTomato mice and the cell sorting of hypothalamic POMC neurons. (A) Average (± SEM) 24 h caloric intake (kcal) of the regular diet (RD) group and the high-fat diet (HFD) group mice. (B) Body weight of the RD group and the HFD group mice. (C) Body weight

gain of the RD group and the HFD group mice. (D) Abdominal white fat of the RD group and the HFD group mice. (E) The quantification of abdominal white fat of the RD group and the HFD group mice. The flow cytometric sorting of hypothalamic neurons from Pomccre-; ROSAtdTomato mice (F) and Pomc-Cre+; ROSA-tdTomato mice (G). (H) The enrichment of Pomc and tdTomato genes in sorted tdTomato+ cells (P3 of Fig.1G) as compared to non-sorted cells (P1 in Fig.1G)

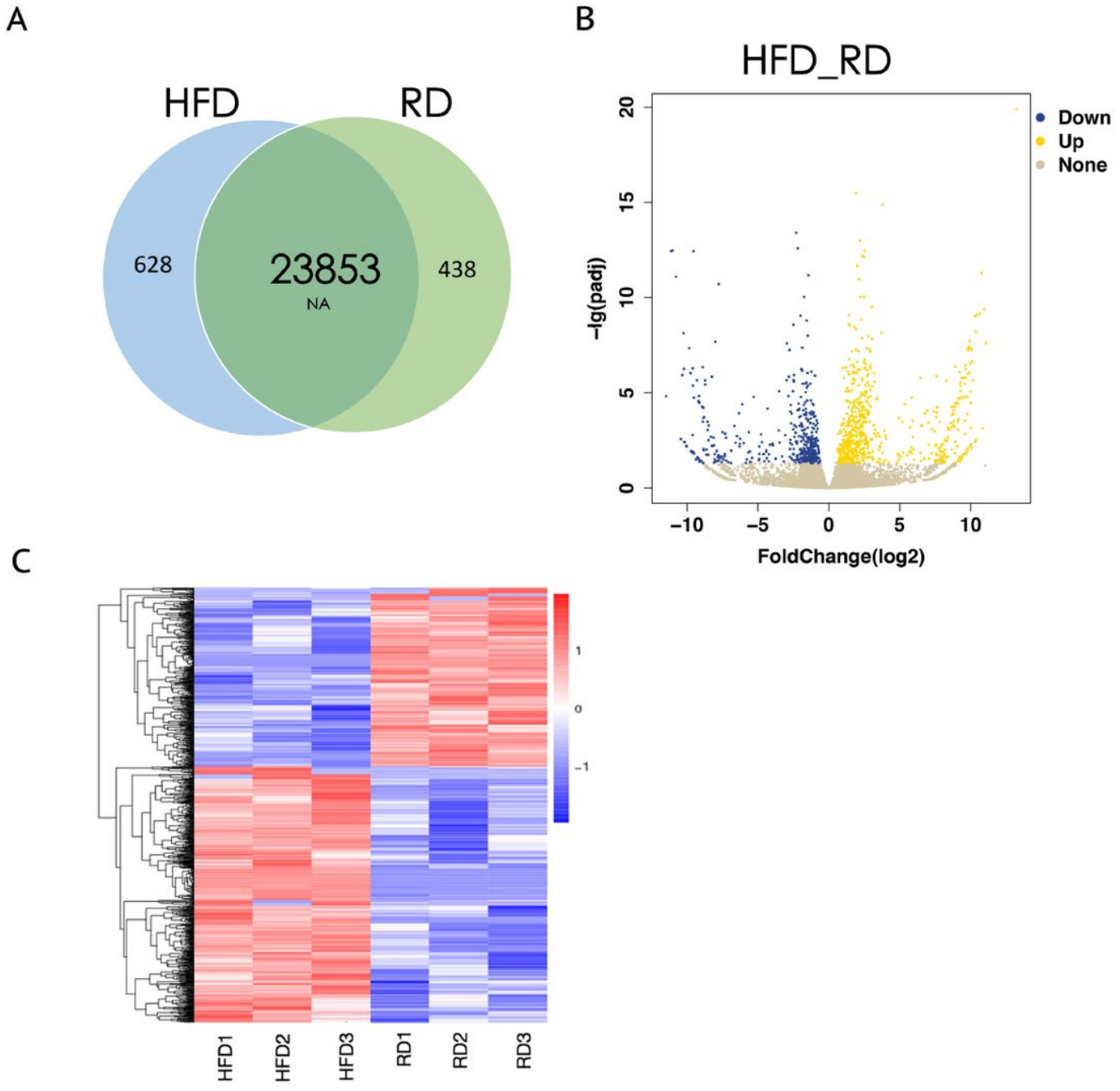

Figure 2

The analysis results of differentially expressed genes. (A) Venn diagram for DEG between HFD group and RD group (Upregulated in HFD: blue, Upregulated in RD: green). Reported DEGs required q-value <0.05, abs[log2(fc)] > 1. (B) The volcano map of differentially expressed genes. NA means no significant change

between HFD and RD. (C) The clustering map of differentially expressed genes. HFD indicated high fat diet group, and RD indicated regular diet group.

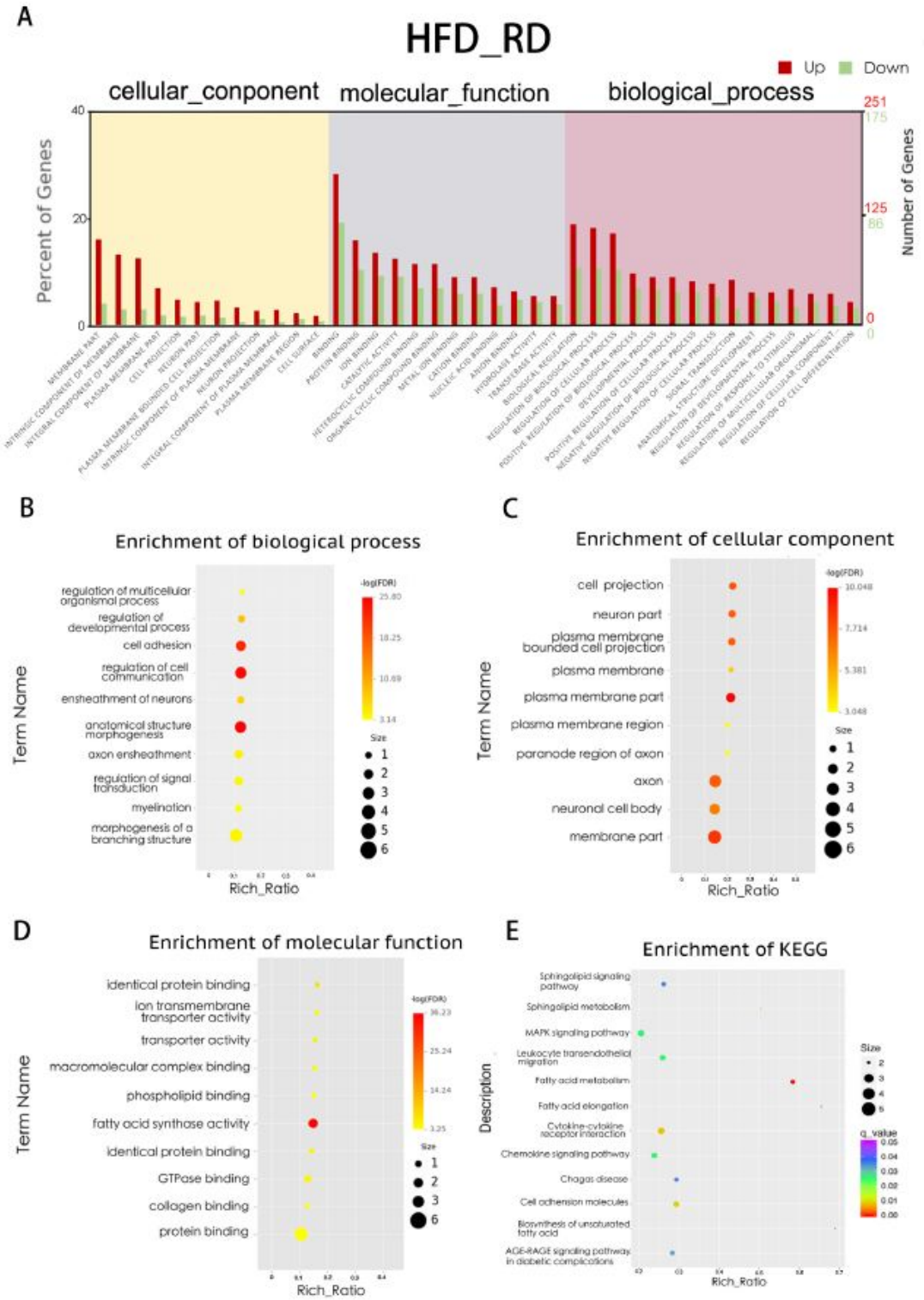

Figure 3

Functional analysis of differentially expressed gene (DEG) in POMC neurons of HFD group compared to RD group. (A) GO functional classification of DEGs according to the enriched gene numbers. (corrected P value < 0.05). Top enriched GO terms of 17 cellular components, 25 molecular functions and 12

biological processes were shown. (B-D) The significant pathway enrichment in GO cellular components, biological process, and molecular functions pathways according to the Bonferroni corrected False Discovery Rate (FDR) and gene counts. (E) The significant KEGG pathway enrichment. Gene counts and p-value corrected by Bonferroni are shown.

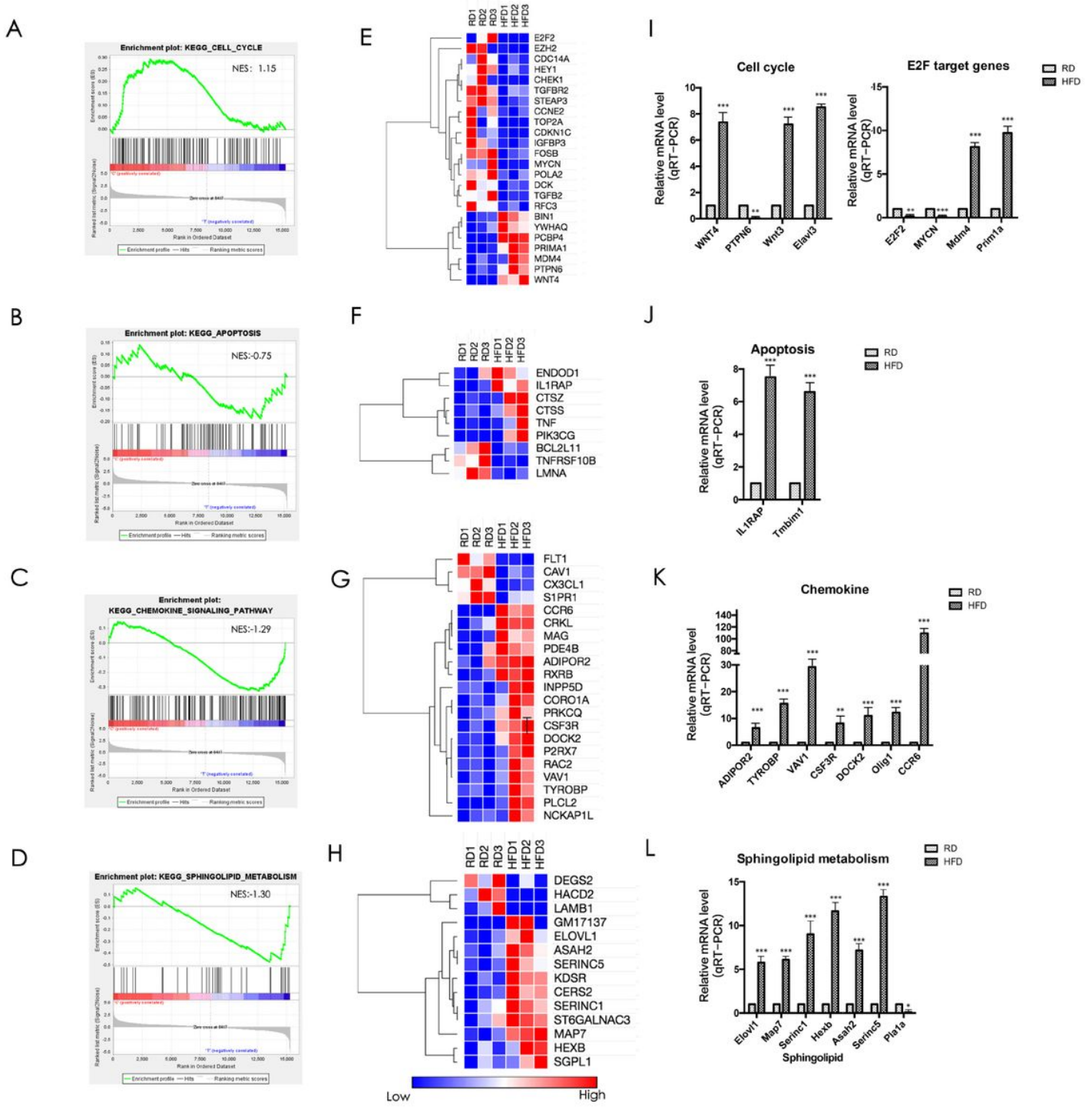

Figure 4

Pathway correlation analysis and RT-qPCR validation of differentially expressed genes (DEGs) of POMC neurons in HFD group compared to RD group. (A-D) The GSEA plots showing the enrichment of indicated

gene set categories of identified DEGs. NES: normalized enrichment score. Positive NES indicates enrichment of gene signatures in HFD group, negative NES indicates enrichment of gene signatures in RD group. (E-H) The expression heatmaps and clustering of identified DEGs, classified belonging to indicated KEGG pathways. Red signal denotes higher abundance, while blue signal denotes lower abundance. (I-L) The RT-qPCR validation of selected DEGs belonging to related KEGG pathways as in plots E-H. "*", "**" and "***" indicated $p < 0.05$, $p < 0.01$ and $p < 0.001$, respectively. The representative KEGG pathways were shown: pathway of cell cycle genes and E2F targets (A, E, I), pathway of apoptosis genes (B, F, J), chemokine signal pathway (C, G, K), pathway of sphingolipid metabolism (D, H, L).

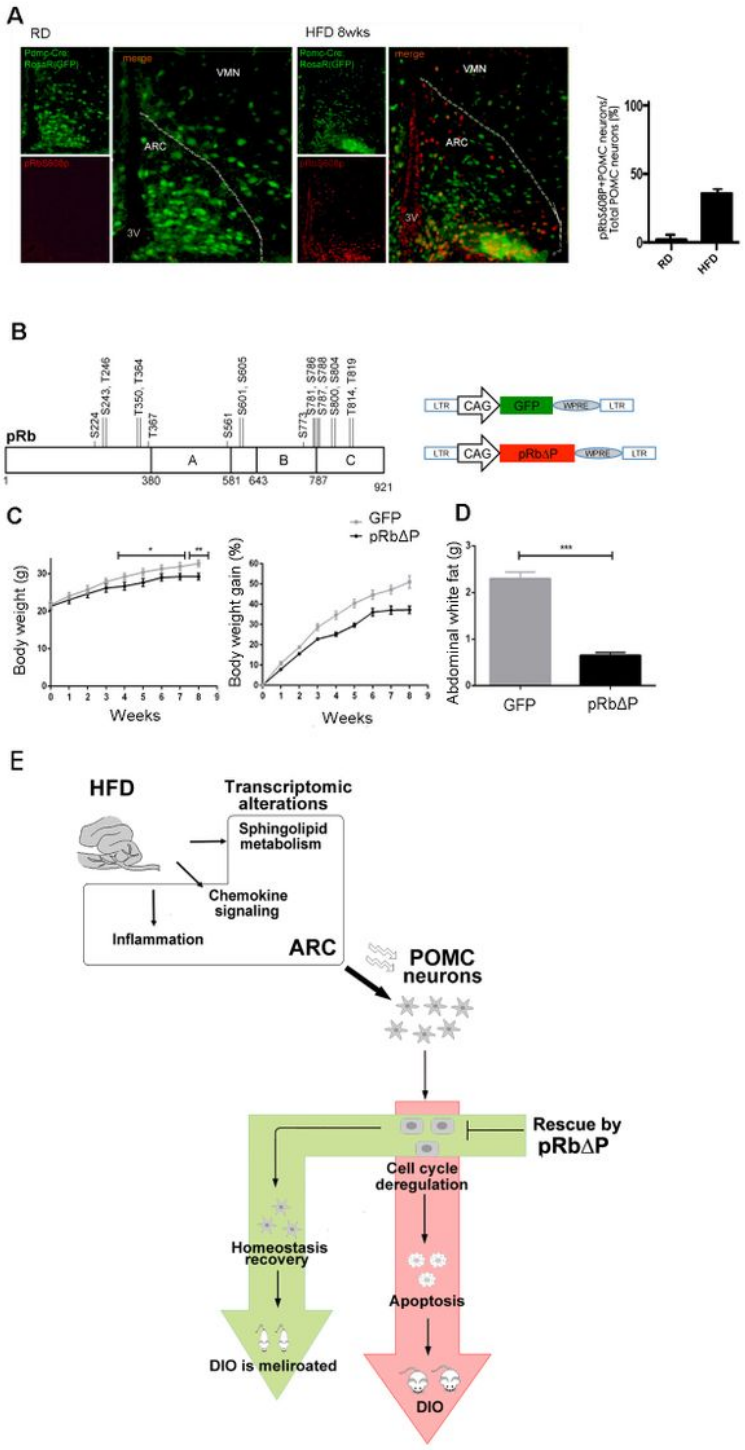

Figure 5

HFD induced phosphorylation of pRb in POMC neurons and stereotaxic injection of unphosphorylated pRb in ARC meliorated the HFD induced DIO. (A) ARC sections from Pomc-Cre; RosaR(GFP) mice in RD and HFD groups were stained with pRb(S608p). Direct GFP was photographed in green. (B) Phosphorylation sites of pRb protein and the schematic maps of the lenti- GFP and lenti-pRb□P plasmids. (C) Body weights and body weight gains of the HFD fed mice injected with lenti-GFP or lenti-pRb□P

lentivirus in ARC (n=5 for each group) . (D) Abdominal white fat content of HFD fed mice injected with lenti-GFP or lenti-pRb□P lentivirus in ARC (n=5 for each group). (E) Predicted schematic model of HFD induced POMC neuron dysregulation.

Supplementary Files

This is a list of supplementary files associated with this preprint. Click to download.

- SupplementaryFigure3.jpg
- Supplimentaryfile3specificgenesprimerlist.xls
- SupplementaryFigure4.jpg
- Supplimentaryfile2Biologicalfunctionanalysis.xls
- SupplimentaryFigure1.jpeg
- Supplimentaryfigure2.jpg
- Supplimentaryfile1genelist.xlsx